Fractal Hole Growth in Strained Block Copolymer Films

Nagraj Koneripalli,[1,*] Frank S. Bates,[1] and Glenn H. Fredrickson[2]
[1]*Department of Chemical Engineering and Materials Science, University of Minnesota, Minneapolis, Minnesota 55455*
[2]*Department of Chemical Engineering, University of California, Santa Barbara, California 93106*
(Received 26 November 1997)

The evolution of surface topography in conformationally strained diblock copolymer films comprised of 3/2 lamellar bilayers was investigated by optical microscopy. Films of thickness $1.25D^* < L < 1.5D^*$ developed two-dimensional isotropic fractal holes with $d_f = 1.67$ following heterogeneous nucleation, where D^* is the equilibrium lamellar spacing. A microscopic theory is presented that maps this hydrostatic tension driven hole growth instability onto the classical description of pattern formation during solidification. [S0031-9007(98)07044-6]

PACS numbers: 61.41.+e, 61.43.Hv, 68.35.Bs, 68.55.Jk

The development of ramified structures as a consequence of interfacial instability is a ubiquitous nonequilibrium phenomenon. Viscous fingering in fluid flow [1], dendritic crystal growth [2], electrodeposition [3], and coral formation are representative of a broad class of patterning processes governed by a competition between diffusion limited transport (e.g., heat or mass) and interfacial tension. In the absence of an intrinsic broken symmetry, the resulting objects often display a fractal morphology characterized by a power-law scaling of density with size that depends on the dimensionality of growth [4]. Connecting the microscopic and macroscopic aspects of fractal formation presents a basic challenge in establishing the universal nature of this class of structural order.

While investigating the development of surface topography in conformationally strained block copolymer thin films [5], we recently observed a new mechanism of hole growth that produces fractal patterns that are remarkably similar to those found in seemingly unrelated systems. This Letter describes our experimental discovery along with a theoretical analysis that accounts for the microscopic origins of the associated two-dimensional fractal objects.

Diblock copolymers are long molecules composed of two linear sequences of chemically distinct repeat units that can self-assemble to form nanoscale, spatially periodic, composition patterns [6]. Symmetric diblocks, constructed from equal size blocks, segregate to form an alternating layered (i.e., lamellar) morphology with a periodicity D^* that is controlled by the overall molecular size. When cast into thin films, the tendency to preserve this layered morphology leads to quantized periodic structures that are either integral (n) or half integral $(1/2 + n)$ in the number of bilayers; symmetric (n) versus asymmetric $(1/2 + n)$ film formation is controlled by the wetting preference of each block [7]. Figure 1 illustrates the free energy for the asymmetric case as a function of the overall film thickness L, based on a self-consistent mean-field calculation [8]; we have ignored surface free-energy effects in this illustration for simplicity. As L increases, the polymer coils are alternatively stretched, then compressed as the number of bilayers increases from 1/2 to 3/2 to 5/2. The minimum free energy for each quantized structure occurs at $L/D^* = 1/2 + n$. Experiments with confined block copolymer thin films of uniform thickness have confirmed this general picture [5,9,10].

Films that have a free surface (e.g., with air) are not constrained to maintain a uniform overall thickness. Therefore, if initially prepared with $L/D^* \neq (1/2 + n)$, islands or holes will develop, splitting the film into two quantized regions, each satisfying $L/D^* = (1/2 + n)$ [11,12]. This process resembles phase separation in bulk

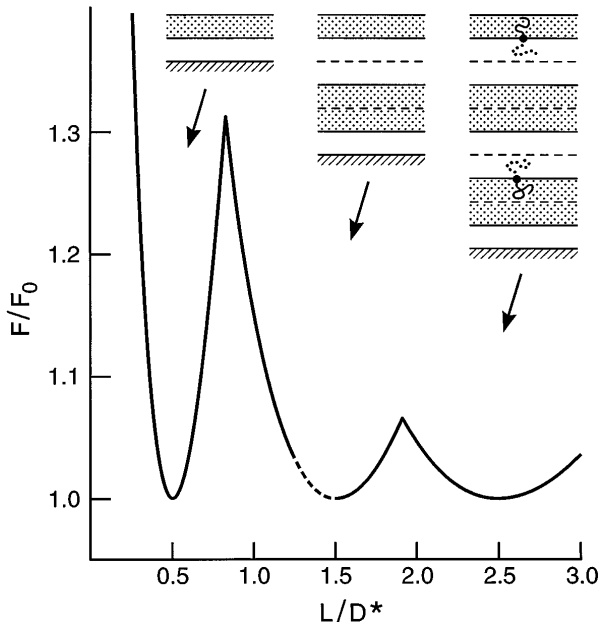

FIG. 1. Calculated lamellar thin-film free energy, relative to the bulk ($L \to \infty$), based on mean-field theory [8]; perturbations due to surface interactions have been ignored for simplicity. Equilibrium thicknesses for unconfined films coincide with local minima. Dashed section at $1.25 < L/D^* < 1.5$ identifies initial states that produced fractal holes.

binary mixtures after cooling into a two-phase region from a homogeneous state.

Uniform strained films (i.e., $L/D^* \neq 1/2 + n$) were prepared from a nearly monodisperse symmetric poly(styrene)-poly(vinylpyridine) (PS-PVP) diblock copolymer ($M_n = 16\,300$ g/mol) using a recently described confinement technique [5]. Prescribed amounts of diblock were spin cast from solution onto oxide-etched silicon wafers, coated with a layer of poly(2-methylvinylcyclohexane) (P2MVCH), then annealed at 140 °C; this is well above the glass transition temperature of PS and PVP ($T_g \cong 100$ °C), but below that of P2MVCH ($T_g \cong 186$ °C). In this Letter we focus on $1.25 < L/D^* \leq 1.60$, which resulted in confined lamellar films containing 1.5 bilayers (see Fig. 1). After annealing, the specimens were cooled to room temperature and the P2MVCH layer was stripped using a selective solvent leaving a smooth, strained, but frozen lamellar morphology with PS and PVP at the air and substrate surfaces, respectively [5]. Subsequent reannealing of these films produced the effects described in the remainder of this Letter.

Figure 2 depicts optical micrographs (reflection mode) that illustrate the temporal evolution of surface topography that occurred when conformationally compressed ($L/D^* = 1.45$) and stretched ($L/D^* = 1.6$) films were reannealed at 140 °C. For $L/D^* = 1.6$ a population of homogeneously distributed $5/2$ bilayer islands appeared dispersed on a sea of $L/D^* = 3/2$ lamellae soon after raising the temperature above T_g. Subsequent island coalescence was extremely slow. A qualitatively different picture emerged from the $L/D^* = 1.45$ film where nucleation and growth of $1/2$ bilayer holes occurred within the $3/2$ layer matrix over a much longer time span. In this case, every isolated hole clearly originated from small heterogeneities (i.e., dirt) on the film. We attribute this transition to heterogeneous nucleation to the enormous free-energy barrier between $L/D^* = 0.5$ and 1.5, relative to that separating $L/D^* = 1.5$ and 2.5 (see Fig. 1), which likely suppresses the rate of homogeneous nucleation. Experiments with $5/2$ bilayer films [13] that nucleate both holes ($L/D^* < 2.5$) and islands ($L/D^* > 2.5$) homogeneously support this hypothesis. The remainder of this Letter focuses on the fractal patterns that emerged in the heterogeneously nucleated $1.25 < L/D^* < 1.5$ films (dashed section in Fig. 1).

An optical micrograph of an isolated fully developed hole is shown in Fig. 3. The fractal dimension of the hole was calculated by the box count method [14] yielding $N(l) \sim l^{-d_f}$ where $N(l)$ is the number of boxes of size l that contain at least part of the object with fractal dimension d_f. Analysis of many such holes yielded $d_f = 1.67 \pm 0.01$ in exact agreement with the theoretical result of Muthukumar [15], $d_f = (d^2 + 2)/(d + 1)$, where $d = 2$ is the space dimension. Our fractal holes are remarkably similar in form to patterns produced during a variety of other nonequilibrium processes [4,14], notably, experiments on fluid flow in Hele-Shaw cells [3] and two-dimensional crystallization on roughened surfaces [2].

We now discuss the origins of the fingering patterns depicted in Figs. 2 and 3. While analyses similar to the one presented here have appeared previously in the literature to describe draining and rupture of thin liquid films [16], as well as dewetting of thin smectic films [17], the present approach makes explicit contact with models of crystallization. It is this latter connection that allows us to conclude that the fractal pattern formation observed in thin block copolymer films is intimately related to a general class of fingering, Laplacian growth systems. By reference to the film free energy shown in Fig. 1, it is clear that films with uniform thicknesses h_∞ in the range $1.25 < L/D^* < 1.5$ are subject to hydrostatic *tension*.

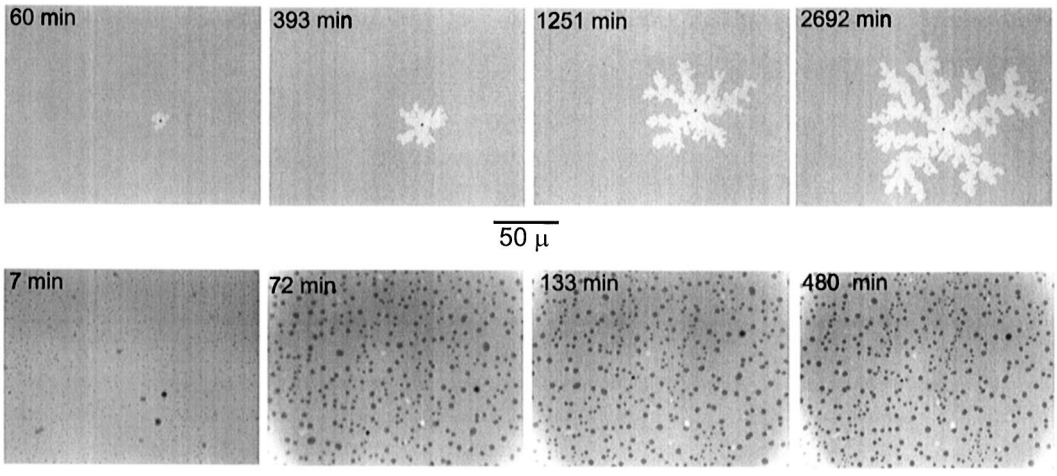

FIG. 2. Temporal evolution of islands ($L/D^* = 1.60$, lower panels) and a hole ($L/D^* = 1.45$, upper panels) during annealing of strained films at 140 °C. Light and dark regions contain 0.5 and 1.5 bilayers (upper panels) and 1.5 and 2.5 bilayers (lower panels), respectively.

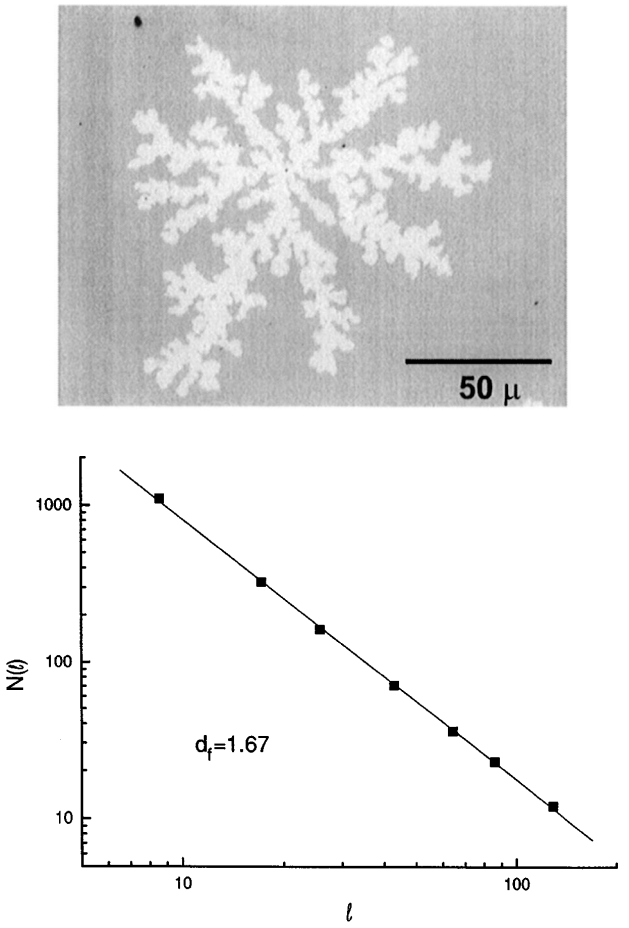

FIG. 3. Analysis of the fractal dimension of a fully developed hole (shown above) grown from an initial film thickness of $L/D^* = 1.40$. A fractal dimension of $d_f = 1.67$ is obtained using the box count method [14] where $N(l)$ is the number of boxes of size l.

Indeed, the pressure inside the film can be expressed as

$$P = P_a - B(h_0 - h_\infty)/h_0\,, \tag{1}$$

where P_a is the ambient pressure, $h_0 = 1.5D^*$ is the film height of the closest free energy minima, and B is the compressional modulus of the lamellar (smectic) film. This tension provides the driving force for nucleation and growth of holes in the surface of the film. We ignore van der Waals interactions in the present analysis because they can be shown to be negligible compared with the elastic strain energy.

In order to describe the time evoluation of a hole that is nucleated about a localized impurity in the film, it is convenient to introduce a function $h(r,t)$ that describes the film thickness (height) at location $\mathbf{r} = (x, y, 0)$ in the substrate plane. As schematically depicted in Fig. 4, this function rises smoothly from a value of $h_H = 0.5D^*$ in the interior of a hole to a maximum value near $h_0 = 1.5D^*$ just outside the hole, and ultimately decays to the value h_∞ constrained by the amount of material deposited on the substrate. Clearly, as a hole grows, polymer must

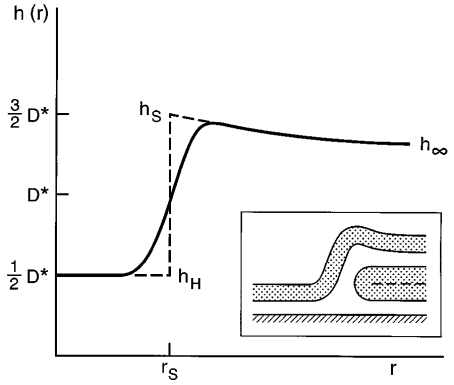

FIG. 4. Illustration of film structure near the edge of a hole. Inset shows the edge defect morphology that produces the height function $h(r)$ given by the solid curve. The dashed curve represents the function used in modeling hole growth.

be transported from the bulge at the periphery of the hole out towards the bulk of the film. The inset shows the smectic defect (edge dislocation) expected at the boundary of the hole. As the length scale over which $h(r,t)$ varies at the hole edge is experimentally much smaller than the scale over which the film height decays to h_∞, it proves mathematically convenient to approximate the hole boundary as a discontinuous step from a film height of h_H inside the hole to a film height of h_S just outside the hole (cf. Fig. 4). While h_S is expected to be numerically close to h_0, we shall see that its value is determined by a type of Laplace-Young condition at the hole boundary.

Next, we turn to deriving an equation of motion for $h(\mathbf{r},t)$ in the region of the film exterior to a hole. Hole advancement results from pressure-driven flow of copolymer in the plane of the film. Assuming no slip boundary conditions at the substrate surface ($z = 0$) and free (vanishing shear stress) boundary conditions at the top of the film [$z = h(\mathbf{r},t)$], the local velocity field is given by (lubrication approximation)

$$\mathbf{u}(\mathbf{r},z;t) = (1/2\eta)\,(z^2 - 2zh)\nabla P\,, \tag{2}$$

where η is the layer sliding viscosity (η_3 in smectic A terminology [18]) and ∇P is the driving pressure gradient in the plane of the film. Combining this result with the continuity equation for an incompressible fluid and integrating over the height of the film yields

$$\partial_t h = (1/3\eta)\nabla \cdot (h^3 \nabla P)\,. \tag{3}$$

We close this equation for $h(\mathbf{r},t)$ with an "equation of state" that relates the local pressure in the film to a sum of ambient, Laplace-Young, and smectic elastic terms, respectively,

$$P(\mathbf{r},t) = P_a - \gamma\nabla^2 h + B[h(\mathbf{r},t) - h_0]/h_0\,, \tag{4}$$

where γ is the air-polymer surface tension.

At the edge of the hole (step), mass conservation leads to the following boundary condition relating the interfacial velocity, v_n, to the normal component of the

pressure gradient at the step (**n** denotes the outward normal to the hole):

$$v_n(h_S - h_H) = -(1/3\eta)h_S^3 \mathbf{n} \cdot \nabla P|_S . \quad (5)$$

A second boundary condition results from a force balance at the step,

$$P_a = P_S + \bar{\gamma}\kappa , \quad (6)$$

where $\kappa = \nabla \cdot \mathbf{n}$ is the curvature of the edge of the hole in the plane of the film. The interfacial tension appearing in this Laplace-Young type equation, $\bar{\gamma}$, should reflect not only the air-polymer tension associated with the step, but also the elastic forces of the edge dislocation. The latter, however, can be argued to scale with the PS-PVP interfacial tension, which is smaller than the air-polymer tension by a factor of $\sqrt{\chi} \ll 1$ where χ is the segment-segment interaction energy parameter [6]. Thus, we assume that $\bar{\gamma} \approx \gamma$.

Our final step is to assume (supported by Fig. 2) that any pattern formation (fingering) occurs on large scales compared with either h_0 or the "capillary length" $d_0 \equiv \gamma/B$, which amounts to neglect of the Laplace-Young term in Eq. (4). A simple rescaling of the film height field to $\psi(\mathbf{r}, t) \equiv [h(\mathbf{r}, t) - h_\infty]/h_\infty$ then yields an evolution equation and boundary conditions closely related to the two-dimensional, "one-sided" model of crystal growth from an undercooled melt [19],

$$\partial_t \psi = D\nabla^2 \psi , \quad (7)$$

$$\psi_S = \Delta - d_0(h_0/h_\infty)\kappa , \quad (8)$$

$$v_n = -1.5(h_0/h_\infty)^2 D \mathbf{n} \cdot \nabla\psi|_S . \quad (9)$$

In the present situation, the "diffusion coefficient" is given by $D \equiv h_\infty^3 B/(3\eta h_0)$ and the dimensionless "undercooling" is small: $\Delta \equiv (h_0 - h_\infty)/h_\infty \approx 0.07$. The first boundary condition in Eq. (8) evidently plays the role of the Gibbs-Thompson relation in crystal growth, while the second boundary condition substitutes for an expression of heat flow conservation.

Having mapped the hole growth kinetics onto a well-studied model of crystal growth, we can exploit a vast literature of theoretical and experimental results on instabilities and pattern formation during solidification [20]. In the limit of an *isotropic* surface tension (i.e., asymmetry strength $\epsilon = 0$), current theory [20] anticipates growth of an open fractal morphology with $d_f = 5/3$ [15,21], consistent with our observation. Thus, fractal hole formation in strained block copolymer films appears to belong to the general class of systems governed by Laplacian growth that includes viscous fingering [1], dendritic crystallization [19], and diffusion limited aggregation [15,22]. Future applications of thin block copolymer films may benefit from this connection, as controlled nucleation and growth processes provide one route to pattern development in this class of materials.

We have derived valuable insights from discussions with David Morse and Rasti Levicki for which we are grateful. This work was supported by the National Science Foundation under Grants No. NSF-DMR 945101 and No. NSF-DMR 9505599, and N. K. received support from the Graduate School at the University of Minnesota.

*Present address: Science Research Laboratory, 3M Company, St. Paul, Minnesota 55144.

[1] G. Daccord, J. Nittmann, and H. E. Stanley, Phys. Rev. Lett. **56**, 336 (1986).
[2] H. Honjo, S. Ohta, and M. Matsushita, J. Phys. Soc. Jpn. **55**, 2487 (1986).
[3] R. M. Brady and R. C. Ball, Nature (London) **309**, 225 (1984); G. M. Homsy, Annu. Rev. Fluid Mech. **19**, 271 (1987).
[4] T. Vicsek, *Fractal Growth Phenomena* (World Scientific, Teaneck, NJ, 1989).
[5] N. Koneripalli, R. Levicky, F. S. Bates, J. Ankner, H. Kaiser, and S. K. Satija, Langmuir **12**, 6681 (1996).
[6] F. S. Bates and G. H. Fredrickson, Annu. Rev. Phys. Chem. **41**, 525 (1990).
[7] G. J. Kellogg, D. G. Walton, A. M. Mayes, P. Lambooy, T. P. Russell, P. D. Gallagher, and S. K. Satija, Phys. Rev. Lett. **76**, 2503 (1996).
[8] M. S. Turner, Phys. Rev. Lett. **69**, 1788 (1992); D. G. Walton, G. J. Kellogg, A. M. Mayes, P. Lambooy, and T. P. Russell, Macromolecules **27**, 6225 (1994).
[9] P. Lambooy, T. P. Russell, G. J. Kellogg, A. M. Mayes, P. D. Gallagher, and S. K. Satija, Phys. Rev. Lett. **72**, 2899 (1994).
[10] N. Koneripalli, N. Singh, R. Levicky, F. S. Bates, P. D. Gallagher, and S. K. Satija, Macromolecules **28**, 2897 (1995).
[11] M. Maaloum, D. Ausserre, D. Chatenay, G. Caulon, and Y. Gallot, Phys. Rev. Lett. **68**, 1575 (1992).
[12] N. Singh, A. Kudrle, M. Sikka, and F. S. Bates, J. Phys. II (France) **5**, 377 (1995).
[13] N. Koneripalli, Ph.D. thesis, University of Minnesota, 1997.
[14] H. Takayasu, *Fractals in the Physical Sciences*, (Manchester University Press, New York, 1990).
[15] M. Muthukumar, Phys. Rev. Lett. **50**, 839 (1983).
[16] E. Ruckenstein and R. K. Jain, Chem. Soc. Faraday Trans. **70**, 2 (1974).
[17] D. Ausserre, F. Brochard-Wyart, and P.-G. de Gennes, C. R. Acad. Sci. Paris, Ser. IIb **320**, 131 (1995).
[18] P.-G. deGennes and J. Prost, *The Physics of Liquid Crystals* (Oxford University Press, New York, 1993).
[19] J. S. Langer, Rev. Mod. Phys. **52**, 1 (1980).
[20] K. Kassner, in *Science and Technology of Crystal Growth*, edited by J. P. vander Eerden and O. S. L. Bruinsma (Kluwer, Dordrecht, 1995).
[21] A. Arneodo, F. Argoul, Y. Couder, and M. Rabaud, Phys. Rev. Lett. **66**, 2332 (1991).
[22] T. Witten and L. M. Sander, Phys. Rev. Lett. **47**, 1400 (1981).